

Non separable Werner states in spontaneous parametric down-conversion

Marco Caminati, Francesco De Martini, Riccardo Perris, Fabio Sciarrino and Veronica

Secondi

Dipartimento di Fisica and Istituto Nazionale per la Fisica della Materia,

Università "La Sapienza", Roma 00185, Italy

Abstract

The multiphoton states generated by high-gain spontaneous parametric down-conversion (SPDC) in presence of large losses are investigated theoretically and experimentally. The explicit form for the two-photon output state has been found to exhibit a Werner structure very resilient to losses for any value of the gain parameter, g . The theoretical results are found in agreement with the experimental data. The last ones are obtained by quantum tomography of the state generated by a high-gain SPDC.

arXiv:quant-ph/0510153v1 19 Oct 2005

Typeset using REVTeX

I. INTRODUCTION

Entanglement, the non classical correlation between separated quantum systems, represents the physical resource lying at the very basis of quantum information (QI), quantum computation and quantum communication. The current proliferation of relevant applications of quantum entanglement, ranging from the one-way quantum computation [1] to the emerging fields of quantum metrology, lithography, etc. [2] strengthens the need of new flexible and reliable techniques to generate entangled states with increasing dimension.

Entangled photonic qubit pairs generated under suitable phase-matching conditions by the spontaneous parametric down conversion (SPDC) process in a nonlinear (NL) crystal have been central to many applications ranging from teleportation [3] to various quantum key distribution protocols [4]. Today the realization of reliable SPDC sources with large efficiency, i.e. with large "brilliance", able to generate entangled pure states is of key interest as they largely determine the range of applications of the sophisticated optical methods required by modern QI. Recently, high brilliance sources have been realized by using bulk [5–7] and periodically poled [8] NL crystals, and fiber coupled SPDC radiation [9]. The extension of the attained results to higher dimensional QI qubit carriers could lead to new information processing tasks [10] and requires the development of appropriate technological and theoretical tools. Significant results in this field are the SPDC generation of four-photon entangled states with or without "*quantum-injection*" [11–16]. At the same time, the sophisticated level attained by QI processing of photonic qubits has directed a consistent part of the experimental endeavour towards the solution of more technical problems. For instance, since the losses due to the photon transmission represent a restriction to the realization of several QI protocols, classes of entangled states robust against losses have been investigated and a few experimental schemes to generate such states have been proposed [17]. In the case of three qubits, entangled states can be classified as "GHZ-type" or as "W-type", the latter exhibiting a larger robustness in bipartite entanglement [18]. The W-states can be generalized to an arbitrary number of qubits and can be generated efficiently by spontaneous

or stimulated emission in a high gain (HG) regime, i.e. when the parametric "gain" is large: $g \gg 0$. The first experimental realization of 3 photons W-states by spontaneous emission have been recently reported [19,20].

In this framework the investigation of the multiphoton state generated in HG condition is of fundamental importance, both on a conceptual and practical sides, e.g. for non-locality test [21,22] or for QI applications. Recently multiphoton entangled states created by HG SPDC have been observed [23]. The aim of the present paper is to investigate relevant aspects of the output wavefunction of the HG scheme. In Section II, the density matrix representing the 2-photon reduced state arising from HG SPDC after propagation over lossy channels is analyzed theoretically. We find that, for any value of g , the resulting 2-photon state is a "Werner state" [24], i.e., a superposition of a maximally entangled (singlet) state with a fully mixed state. This condition is investigated thoroughly by exploiting the extensive knowledge available on the Werner states and modern techniques like the "entanglement witness" and the various forms of state entropy [25,26]. Resilience of entanglement is theoretically demonstrated for any value of g in the high loss (HL) approximation [27]. In Section III, the results of the theory are compared with the corresponding experimental data obtained by conventional quantum state tomography (QST).

II. SPDC IN HIGH LOSSES REGIME: GENERATION OF WERNER STATES

In this Section, we theoretically analyze the effect of losses on HG SPDC multiphoton state. Recently Durkin *et al.* [27] demonstrated the persistence of some kind of symmetries implying entanglement in multiphoton SPDC states in presence of polarization independent photon losses. Here we explicitly derive the expression of the SPDC density matrix in regime of induced high photon losses through coincidence measurements and demonstrate that it corresponds to a Werner state for any value of g . In the present model effects of both losses and imperfect detections on the output states are simulated, as usual, by the insertion of beam splitters on the two propagation modes \mathbf{k}_i ($i = 1, 2$) (Fig.1). The results

of this study demonstrate the resilience of bipartite entanglement for any value of g . This implies that, even in absence of these induced losses, the initial SPDC state is entangled for any g , because of the basic impossibility of creating or enhancing the entanglement by means of local operations acting on non entangled state [28]. The main motivations for the present investigation resides in the experimental entanglement assessment on multi-photon HG fields by introducing light absorbing filters on the correlated photons paths. The approximate expression of the density matrix also provides an intuitive explanation of the behavior of SPDC states in the HG and HL regimes.

The Hamiltonian of the SPDC process in the interaction picture reads [13,29]

$$\hat{H} = i\kappa(\hat{a}_{1H}^\dagger\hat{a}_{2V}^\dagger - \hat{a}_{1V}^\dagger\hat{a}_{2H}^\dagger) + h.c. \quad (1)$$

where \hat{a}_{ij}^\dagger represents the creation operators associated with the spatial propagation mode \mathbf{k}_i , with polarization $j = \{H, V\}$. H and V stand for horizontal and vertical polarization. κ is a coupling constant which depends on the crystal nonlinearity and is proportional to the amplitude of the pump beam. This Hamiltonian generates a unitary transformation $\hat{U} = e^{-i\frac{\hat{H}t}{\hbar}}$ acting on the input vacuum state $|0\rangle_{1H}|0\rangle_{1V}|0\rangle_{2H}|0\rangle_{2V} = |0, 0, 0, 0\rangle$. The output state $|\Psi^{OUT}\rangle = \hat{U}|0, 0, 0, 0\rangle$ is easily obtained in virtue of the disentangling theorem [30]:

$$|\Psi^{OUT}\rangle = \frac{1}{C^2} \sum_{n=0}^{\infty} \sqrt{n+1}\Gamma^2 |\psi_-^n\rangle \quad (2)$$

where $|\psi_-^n\rangle$ is the n -generated pairs term:

$$|\psi_-^n\rangle = \frac{1}{\sqrt{n+1}} \sum_{m=0}^n (-1)^m |n-m\rangle_{1H} |m\rangle_{1V} |m\rangle_{2H} |n-m\rangle_{2V} \quad (3)$$

and $\Gamma = \tanh g$, $C = \cosh g$. The parameter $g \equiv \kappa t_{int}$ expresses the NL gain of the parametric process, being t_{int} the interaction time. The average number of photon generated per mode is equal to $\bar{n} = \sinh^2 g$.

Let us first consider the contribution $|\psi_-^n\rangle\langle\psi_-^n|$ to the overall density matrix. To investigate the propagation over a lossy channel, a beam splitter(BS) with transmittivity η for any polarization and spatial mode is assumed to simulate the effect of channel losses and

of detector inefficiencies. Furthermore, perfect detectors with $\eta_{QE} = 1$ measure the output state [31] (Fig.1). The symmetry of the entangled state after losses is preserved by assuming η to be mode- and polarization- independent. The contribution $|\psi_-^n\rangle$ to the SPDC state is expressed in terms of the BS operators $\{\hat{a}_{ij-IN}^\dagger\}$ associated with the input modes $\{\mathbf{k}_i^{IN}\}$:

$$|\psi_-^n\rangle = \frac{1}{\sqrt{n+1}} \frac{1}{n!} (\hat{a}_{1H-IN}^\dagger \hat{a}_{2V-IN}^\dagger - \hat{a}_{1V-IN}^\dagger \hat{a}_{2H-IN}^\dagger)^n |0, 0, 0, 0\rangle \quad (4)$$

The BS's couple the input modes $\{\mathbf{k}_i^{IN}\}$ with the transmitted modes $\{\mathbf{k}_i^{OUT}\}$ and the reflected modes $\{\tilde{\mathbf{k}}_i^{OUT}\}$. The output state expression is found by substituting the operators $\{\hat{a}_{ij-IN}^\dagger\}$ with their expressions in term of the operators $\{\hat{a}_{ij-OUT}^\dagger\}$, associated with the output transmitted modes $\{\mathbf{k}_i^{OUT}\}$, and the operators $\{\hat{b}_{ij-OUT}^\dagger\}$, associated with the output reflected modes $\{\tilde{\mathbf{k}}_i^{OUT}\}$, through the BS input-output matrix [31]:

$$\begin{pmatrix} \hat{a}_{ij-OUT}^\dagger(t) \\ \hat{b}_{ij-OUT}^\dagger(t) \end{pmatrix} = \begin{pmatrix} \sqrt{\eta} & i\sqrt{1-\eta} \\ i\sqrt{1-\eta} & \sqrt{\eta} \end{pmatrix} \begin{pmatrix} \hat{a}_{ij-IN}^\dagger(t) \\ \hat{b}_{ij-IN}^\dagger(t) \end{pmatrix} \quad (5)$$

The input state $|\psi_-^n\rangle$ evolves into an output state $|\psi_-^n\rangle^{OUT}$ which is defined over the four transmitted modes and the four reflected modes. This state is expressed through the Fock states: $|n_{1H}, n_{1V}, n_{2H}, n_{2V}\rangle_a \otimes |n_{1H}, n_{1V}, n_{2H}, n_{2V}\rangle_b$ where the first term in the tensor product represents modes transmitted by the BS and hence detected (\hat{a} -modes) while the second term expresses the reflected modes (\hat{b} -modes).

The density matrix $\sigma^{OUT} = [|\psi_-^n\rangle \langle \psi_-^n|]^{OUT}$ of the n -pair term of the SPDC state can be easily obtained from the previous expressions:

$$\begin{aligned} [|\psi_-^n\rangle \langle \psi_-^n|]^{OUT} &= \frac{1}{n+1} \left(\frac{1}{n!}\right)^2 \sum_{k,l_i} \sum_{h,f_j} A^*(h, \{f_j\}) A(k, \{l_i\}) * \\ &* |l_1, l_2, l_3, l_4\rangle_a \otimes |n-k-l_1, k-l_2, k-l_3, n-k-l_4\rangle_b * \\ &* {}_a \langle f_1, f_2, f_3, f_4 | \otimes {}_b \langle n-h-f_1, h-f_2, h-f_3, n-h-f_4 | \end{aligned} \quad (6)$$

with

$$\begin{aligned} A(x, \{y_k\}) &= \binom{n}{x} \binom{n-x}{y_1} \binom{x}{y_2} \binom{x}{y_3} \binom{n-x}{y_4} (-1)^x \eta^{y_1+y_2+y_3+y_4} (-i\sqrt{1-\eta})^{2n-y_1-y_2-y_3-y_4} * \\ &* \sqrt{y_1!(n-x-y_1)!y_2!(x-y_2)!y_3!(x-y_3)!y_4!(n-x-y_4)!} \end{aligned} \quad (7)$$

and $\sum_{x,y_i} \equiv \sum_{x=0}^n \sum_{y_1,y_4=0}^{n-x} \sum_{y_3,y_2=0}^x$. Since we are interested in the reduced density matrix ρ_a^n defined over the transmitted modes $\{\mathbf{k}_i^{OUT}\}$, $\rho_a^n = Tr_b [|\psi_-^n\rangle\langle\psi_-^n|]^{OUT}$, we need to trace σ^{OUT} over the undetected reflected modes. The result is:

$$\rho_a^n = \frac{1}{n+1} \left(\frac{1}{n!}\right)^2 \sum_{k,l_i} \sum_{h,f_j} A^*(h, \{f_j\}) A(k, \{l_i\}) |l_1, l_2, l_3, l_4\rangle_{aa} \langle f_1, f_2, f_3, f_4| \quad (8)$$

$$* \delta(n-k-l_1, n-h-f_1) \delta(k-l_2, h-f_2) \delta(k-l_3, h-f_3) \delta(n-k-l_4, n-h-f_4)$$

The final expression for the n -pair contribution to the SPDC density matrix is:

$$\rho_a^n = \frac{1}{n+1} \sum_{k,l_i} \sum_{h,f_j} (-1)^{k+h} (1-\eta)^{2n} S(h, k, l_2) S(h, k, l_3) \tilde{S}(h, k, l_1) \tilde{S}(h, k, l_4)$$

$$|l_1, l_2, l_3, l_4\rangle \langle k-h+l_1, h-k+l_2, h-k+l_3, k-h+l_4|$$

where $S(h, k, p) = \zeta^p \sqrt{\binom{k}{p} \binom{h}{k-p}}$, $\tilde{S}(h, k, p) = \zeta^p \sqrt{\binom{n-k}{p} \binom{n-h}{k-h+p}}$ and $\zeta = \frac{\eta}{1-\eta}$.

Up to now we have considered arbitrary, polarization-symmetric losses. In the following we make the additional assumption of very large losses, i.e. HL, which greatly simplifies our task. Such approximation is expressed by the relation $\eta\bar{n} \ll 1$, $\eta\bar{n}$ being the average number of photon transmitted by the BS per mode. This condition enables us to take into account only the terms of the sum Eq.7 of order $\leq \eta^2$, hence considering only matrix element corresponding to no more than two photons transmitted. As final step, we assume to detect one photon on each mode \mathbf{k}_i^{OUT} by a 2-photon coincidence technique. In this way the vacuum terms affecting one or both vectors \mathbf{k}_i^{OUT} are dropped. In summary, this coincidence procedure guarantees, by post-selection, that we are dealing only with matrix elements arising from the tensor product of the states: $\{|1, 0, 1, 0\rangle, |1, 0, 0, 1\rangle, |0, 1, 1, 0\rangle, |0, 1, 0, 1\rangle\}$, which correspond to the states $\{|H\rangle_1 |H\rangle_2, |H\rangle_1 |V\rangle_2, |V\rangle_1 |H\rangle_2, |V\rangle_1 |V\rangle_2\}$. The n -pair contribution ρ_{post}^n to the SPDC 2-photon density matrix hence reads

$$\rho_{post}^n = \frac{1}{6} n (1-\eta)^{2n} \zeta^2 \begin{pmatrix} (n-1) & 0 & 0 & 0 \\ 0 & (1+2n) & -(n+2) & 0 \\ 0 & -(n+2) & (1+2n) & 0 \\ 0 & 0 & 0 & (n-1) \end{pmatrix} \quad (10)$$

We note that the above density matrix has the form of a Werner state $\rho_W = p |\Psi_-\rangle \langle \Psi_-| + \frac{1-p}{4} I$, with $p = \frac{(n+2)}{3n}$ which is a mixture with probability p of the maximally entangled state $|\Psi_-\rangle = 2^{-1/2}(|H\rangle_1 |V\rangle_2 - |V\rangle_1 |H\rangle_2)$ and of the maximally chaotic state $I/4$ being I the identity operator on the overall Hilbert space. These states are commonly adopted in QI, since they model a decoherence process occurring on a singlet state traveling along an isotropic noisy channel [32].

The complete density matrix for the SPDC output state is obtained by substituting the ρ_{post}^n matrices into the expression $\rho_{th}^{II} = \frac{1}{C^4} \sum_{n=0}^{\infty} (n+1) \Gamma^{2n} \rho_{post}^n$. All the terms ρ_{post}^n sum up incoherently. Let us explain the latter procedure. In the actual conditions any $[[\psi_-^n] \langle \psi_-^n|]$ leads, after the BS action, to two transmitted photons and $2(n-1)$ reflected photons. Different n number of input pairs lead to the discard of a different numbers of reflected photons, hence any mutual coherence is destroyed after the tracing operation. The normalized density matrix turns out to be:

$$\rho_{th}^{II} = \begin{pmatrix} \frac{1-p}{4} & 0 & 0 & 0 \\ 0 & \frac{1+p}{4} & -\frac{p}{2} & 0 \\ 0 & -\frac{p}{2} & \frac{1+p}{4} & 0 \\ 0 & 0 & 0 & \frac{1-p}{4} \end{pmatrix} \quad (11)$$

The SPDC density matrix ρ_{th}^{II} , given by the sum of Werner states, is a Werner state itself, with singlet weight

$$p = \frac{1}{2\tilde{\Gamma}^2 + 1} \quad (12)$$

with $\tilde{\Gamma} = (1-\eta) \tanh g$. In the limit $\eta \rightarrow 0$, $\tilde{\Gamma} = \tanh g$. For large values of g , i.e. for $\tilde{\Gamma} \rightarrow 1$, and in the hypothesis of very high losses, the singlet weight $p \geq \frac{1}{3}$ approaches the minimum value $\frac{1}{3}$. Since the condition $p > \frac{1}{3}$ implies the well known non-separability condition for a general Werner state, we have demonstrated for large g the expected high resilience against de-coherence of the entangled singlet state [24]. The graph of Fig.2 shows the behavior of singlet weight p as a function of the interaction parameter g .

III. EXPERIMENTAL REALIZATION

The previous theoretical results have been experimentally tested for different values of the parametric NL-gain g : Fig.3. The main source was a *Ti : Sa Coherent MIRA* mode-locked laser further amplified by a *Ti : Sa regenerative Coherent Rega 9000* device (A) operating with pulse duration $180fs$. The amplifier could operate either at a repetition rate $250kHz$ or $100kHz$ leading to an energy per pulse, respectively, of $4\mu J$ and $8\mu J$. The output beam was frequency doubled in a UV beam at $\lambda_p = 397.5nm$ through a *Second Harmonic Generation (SHG)* process, achieved by focusing the infrared beam into a $1mm$ thick BBO crystal (β - barium - borate), cut for type I phase matching, through a lens with focal length of $20cm$. The nonlinear (NL) crystal was placed at $5cm$ from the beam waist in order to avoid crystal damage and beam spatial distortion. The UV beam then excited a *SPDC* process in a $L = 1.5mm$ thick BBO NL crystal slab: Fig. 3. The *SPDC*-generated photons with degenerate wavelengths (wl's) $\lambda = 2\lambda_p = 795nm$ propagated along the \mathbf{k}_1 and \mathbf{k}_2 modes. A $\lambda/2$ waveplate (wp) and a $\frac{L}{2}$ thick BBO were placed on each mode to ensure the accurate compensation of all residual birefringence effects coming from the main BBO crystal, cut for type II phase matching [5]. In each mode \mathbf{k}_i , an additional glass plate (G_p) ensured a tight balance between the two polarization emission cones of the SPDC process. The balancement between the two cones was achieved by suitable tilting of G_p in order to vary the ratio between the transmittivities for the s - and p -polarized waves. Calibrated neutral attenuation filters (At) placed in modes \mathbf{k}_1 and \mathbf{k}_2 were adopted to assure the condition of high-losses and hence single-photon detection regime. The polarization states analysis was carried out through two π -analyzers (T_1 and T_2 in Fig.3) each one consisting of a pair of $\lambda/4 + \lambda/2$ optical waveplates, a polarizing beam splitter (PBS), a single mode fiber coupled detector *SPCM - AQR14 - FC* with an interferential filter of bandwidth $\Delta\lambda = 4.5nm$ placed in front of it. The combination of the UV $\lambda/2$ wp (WP_P) and PBS_P allowed a fine tuning of the UV pump power exciting the NL crystal.

In a first experiment we estimated the gain value (g) of the optical parametric process

and the overall quantum efficiencies of the detection apparatus on both modes. The count rates of D_1 and D_2 and the coincidence rate $[D_1, D_2]$ were measured for different values of the UV power (Fig.4). The plots of Figure 4-(a) and 4-(b) clearly show the onset of the NL parametric interaction with large g , thus implying the generation of many photon pairs. The gain value of the process is obtained by fitting the count rates N_i of detector D_i , dependent of the UV pump power, with the function $N_i(g) = R \frac{\eta_i \Gamma^2}{1 - (1 - \eta_i) \Gamma^2}$. Here η_i is the quantum efficiency on mode \mathbf{k}_i and R is the repetition rate of the pump source [23]. The maximal value of gain obtained has been found $g_{\max} = (1.313 \pm 0.002)$, which leads to a mean photon number per mode $\bar{n} = \sinh^2 g_{\max} = (2.97 \pm 0.01)$. In conclusion the maximal total number of generated photon on \mathbf{k}_1 and \mathbf{k}_2 modes through the SPDC process is $M = 4\bar{n} = (11.89 \pm 0.05)$. By means of the previous fits we could also estimated the overall detection efficiencies (η_i) on the \mathbf{k}_1 and \mathbf{k}_2 modes which depend on the glass attenuation, the fiber coupling, the detection quantum efficiencies: $\eta_1 = (0.016 \pm 0.002)$ and $\eta_2 = (0.014 \pm 0.002)$. By the previous values we find $\eta\bar{n} \simeq 0.05$.

The main experimental result of the present work is the full characterization of the 2-photon state. We reconstructed the density matrix ρ_{exp}^{II} of the generated 2-qubit state on \mathbf{k}_1 and \mathbf{k}_2 modes by adopting the Quantum State Tomography method (*QST*) [33]. The experimental density matrix ρ_{exp}^{II} is obtained by first measuring the 2-photon coincidences $[D_1, D_2]$ for different settings of the *QST* setup, T_1 and T_2 , and then by applying a numerical algorithm to estimate the density matrix. In a low gain condition the SPDC state generated on \mathbf{k}_1 and \mathbf{k}_2 modes is expected to be in the singlet state $|\Psi^-\rangle = 2^{-1/2} (|H\rangle_{k_1} |V\rangle_{k_2} - |V\rangle_{k_1} |H\rangle_{k_2})$, with excellent agreement between theory and experiment: Figure 5-(**d**). By increasing g , the ρ elements corresponding to $|H\rangle_{k_1} |H\rangle_{k_2}$, $\langle H|_{k_2} \langle H|$ and $|V\rangle_{k_1} |V\rangle_{k_2}$, $\langle V|_{k_2} \langle V|$ are no longer negligible and the detection of two photon with same polarization is a consequence of a multipairs condition: (Figure 5-(**c**), (**b**), (**a**)). The experimental results of the density matrices ρ_{exp}^{II} for different g -values are in good agreement with the theoretical prediction ρ_{th}^{II} ; the mean value of fidelity between the four comparison is $\mathcal{F} = (0.996 \pm 0.002)$, where

$$\mathcal{F}(\rho_{th}^{II}, \rho_{exp}^{II}) = Tr^2 \sqrt{\sqrt{\rho_{th}^{II}} \rho_{exp}^{II} \sqrt{\rho_{th}^{II}}}.$$

The density matrices ρ_{exp}^{II} can now be adopted to estimate "singlet weight", "tangle" and "linear entropy" of the generated state. The density matrix ρ_W of a Werner state is given by the expression (11), as said. The singlet weight (p) can be directly obtained by the matrix elements as $p = (\rho_{exp}^{II})_{22} + (\rho_{exp}^{II})_{33} - (\rho_{exp}^{II})_{11} - (\rho_{exp}^{II})_{44}$. Werner states are entangled ($p > \frac{1}{3}$) or separable ($p \leq \frac{1}{3}$), the extreme conditions being the pure singlet ($p = 1$) and the totally mixed state ($p = 0$). The tangle is a parameter expressing the degree of entanglement of the state, which is defined as $\tau = C^2$, where C is the concurrence of the state [34]; $\tau > 0$ is a necessary and sufficient condition for a 2×2 state to be entangled. Another important property for a mixed state is *linear entropy* (S), which quantifies the degree of disorder, viz. the mixedness of the system. For a system of dimension 4, it results $S = \frac{4}{3}(1 - Tr(\rho^2))$. In case of a Werner state, we have $S_W = (1 - p^2)$. For Werner states, "tangle" and "linear entropy" are found to be related as follows [35]:

$$\tau(S_W) = \begin{cases} \frac{1}{4}(1 - 3\sqrt{1 - S_W})^2 & \text{for } 0 \leq S_W \leq \frac{8}{9} \\ 0 & \text{for } \frac{8}{9} \leq S_W \leq 1 \end{cases} \quad (13)$$

For each experimental value of g , (S, τ) are estimated starting from the experimental density matrix. The agreement between experimental results and theoretical predictions are found satisfactory: Figure 6-(a).

An alternative method to establish whether a state is entangled or not is based on the concept of entanglement witness. A state ρ is entangled if and only if there exists a Hermitian operator \hat{O} , a so-called *entanglement witness*, which has positive expectation value $Tr[\hat{O}\rho_{sep}] \geq 0$ for all separable states ρ_{sep} and has negative expectation value $Tr[\hat{O}\rho] < 0$ on the state ρ [36–39]. For Werner states ρ_W the method proposed in [25,41] leads to the following entanglement-witness operator:

$$\hat{O}_W = \frac{1}{2} \left(\begin{array}{l} |H\rangle|H\rangle\langle H|\langle H| + |V\rangle|V\rangle\langle V|\langle V| + |D\rangle|D\rangle\langle D|\langle D| \\ + |F\rangle|F\rangle\langle F|\langle F| - |L\rangle|R\rangle\langle L|\langle R| - |R\rangle|L\rangle\langle R|\langle L| \end{array} \right) \quad (14)$$

where $|D\rangle = \frac{1}{\sqrt{2}}(|H\rangle + |V\rangle)$ and $|F\rangle = \frac{1}{\sqrt{2}}(|H\rangle - |V\rangle)$ express diagonally polarized single photon states, while $|L\rangle = \frac{1}{\sqrt{2}}(|H\rangle + i|V\rangle)$ and $|R\rangle = \frac{1}{\sqrt{2}}(|H\rangle - i|V\rangle)$ express left and right circular polarization states. The relationship between the expectation value for a Werner state $W_W = Tr[\hat{O}_W \rho_W]$ and the Werner weight p is found to be

$$W_W(p) = \frac{1 - 3p}{4} \quad (15)$$

[7], leading to $W_W(p) < 0$ for $p > \frac{1}{3}$. Experimentally $Tr[\hat{O}_W \rho_{\text{exp}}^{II}]$ has been estimated through 8 projective measurements (the 6 projectors appearing in (14) and the operators $\{|H\rangle\langle V|, |V\rangle\langle H|, |V\rangle\langle V|, |H\rangle\langle H|\}$ for normalization. [26]). In conclusion, for each g value, a point of the Cartesian plane of coordinates (p, W) is obtained: Figure 6-(b). The solid line reports the theoretical dependence (15). The comparison demonstrates a good agreement between the theoretical prediction and experimental results.

By the different methods described above the entanglement condition has been found to be realized for a value of g up to 1.084 ± 0.002 (Fig.5-(c)), corresponding to an average number of photons equal to $M = 4\bar{n} = (6.85 \pm 0.03)$ before losses. For higher values of g the presence of bipartite entanglement is degraded by decoherence effects, mostly due to imperfect correction of the walk-off effect in the BBO crystal and to time distinguishability introduced by the femtosecond pump pulse.

IV. CONCLUSIONS

In summary, the present work shows that the multiphoton states generated by SPDC exhibit a bipartite entanglement even in the presence of high losses, confirming previous analysis [27]. An explicit form has been derived for the output two photon state: a Werner state. The theoretical result are found to be in very good agreement with experimental data. We believe that the present results could be useful to investigate the resilience of entanglement in lossy communication. The present approach can be extended to investigate the *quantum injected optical parametric amplifier (QIOPA)* [42,13,14].

We thank Marco Barbieri for useful discussions. Work supported by the FET EU Network on QI Communication (IST-2000-29681: ATESIT), INFN (PRA "CLON") and by MIUR (COFIN 2002).

REFERENCES

- [1] R. Raussendorf , and H. J Briegel, Phys. Rev. Lett. **86**, 5188 (2001); P. Walther, *et al.*, Nature (London) **434**, 169 (2005).
- [2] A.N. Boto, *et al.*, Phys. Rev. Lett. **85**, 2733 (2000).
- [3] D. Boschi, S. Branca, F. De Martini, L. Hardy, and S. Popescu, Phys. Rev. Lett. **80**, 1121 (1998); D. Bouwmeester, *et al.*, Nature (London) **390**, 575 (1997); E. Lombardi, F. Sciarrino, S. Popescu and F. De Martini, Phys. Rev. Lett. **88**, 070402 (2002).
- [4] N. Gisin, G. Ribordy, W. Tittel., H. Zbinden, Rev. Mod. Phys. **74**, 145 (2002).
- [5] P.G. Kwiat, K. Mattle, H. Weinfurter, and A. Zeilinger, Phys. Rev. Lett. **75**, 4337 (1995).
- [6] P G. Kwiat, E, Waks, A.G. White, I. Appelbaum, and P.H. Eberhard, Phys. Rev. A **60**, R867 (1999).
- [7] C. Cinelli, G. Di Nepi, F. De Martini, M. Barbieri, and P. Mataloni, Phys. Rev. A **70**, 022321 (2004).
- [8] M. Fiorentino *et al.*, Phys. Rev. A **69**, 041801 (2004).
- [9] C. Kurtsiefer, M. Oberparleiter, and H. Weinfurter, Phys. Rev. A **64**, 023802 (2001).
- [10] G.A. Durkin, C.Simon, and D. Bouwmeester, Phys. Rev. Lett. **88**, 187902 (2002).
- [11] F. De Martini *et al.* Optics Comm. **179**, 581 (2000); F. De Martini, *et al.*, Phys. Rev. Lett. **87**, 150401 (2001).
- [12] A. Lamas-Linares, J.C. Howell, and D. Bouwmeester, Nature (London) **412**, 887 (2001); J.C. Howell, A. Lamas-Linares, and D. Bouwmeester, Phys. Rev. Lett. **88**, 030401 (2002).
- [13] D. Pelliccia, V. Schettini, F. Sciarrino, C. Sias, and F. De Martini, Phys. Rev. A **68**,

- 042306 (2003).
- [14] F. De Martini, D. Pelliccia, and F. Sciarrino, Phys. Rev. Lett. **92**, 067901 (2004).
- [15] M. Eibl, S. Gaertner, M. Bourennane, C. Kurtsiefer, M. Zukowski, and H. Weinfurter, Phys. Rev. Lett. **90**, 200403 (2003).
- [16] Z. Zhao, Y.-A. Chen, A.-N. Zhang, T. Yang, H.J. Briegel, and J.-W. Pan, Nature (London) **430**, 54 (2004).
- [17] W. Dür, G. Vidal, and J. I. Cirac, Phys. Rev. A **62**, 062314 (2000).
- [18] A. Acín, D. Bruß, M. Lewenstein, and A. Sanpera, Phys. Rev. Lett. **87**, 040401 (2001).
- [19] M. Eibl, N. Kiesel, M. Bourennane, C. Kurtsiefer, and H. Weinfurter, Phys. Rev. Lett. **92**, 077901 (2004).
- [20] P. Walther, K.J. Resch, and A. Zeilinger, Phys. Rev. Lett. **94**, 240501 (2005).
- [21] M.D. Reid, *et al.*, Phys. Rev. A **66**, 033801 (2002).
- [22] C. Simon and D. Bouwmeester, Phys. Rev. Lett. **91**, 053601 (2003).
- [23] H. S. Eisenberg, G. Khoury, G. A. Durkin, C. Simon, and D. Bouwmeester, Phys. Rev. Lett. **93**, 193901 (2004).
- [24] R. F. Werner, Phys Rev. A **40**, 4277 (1989).
- [25] O. Gühne, *et al.*, Phys. Rev. A **66**, 062305 (2002).
- [26] M. Barbieri, F. De Martini, G. Di Nepi, and P. Mataloni, Phys. Rev. Lett. **91**, 227901 (2003).
- [27] G.A. Durkin, C. Simon, J. Eisert, and D. Bouwmeester, Phys. Rev. A **70**, 062305 (2004).
- [28] V. Vedral and M. B. Plenio, Phys. Rev. A **57**, 1619 (1998).
- [29] F. De Martini and F. Sciarrino, Progress in Quantum Electronics **29**, 165 (2005).

- [30] M.J. Collett, Phys. Rev. A **38**, 2233 (1988).
- [31] R. Loudon, *The Quantum Theory of Light*, 3rd edition, Oxford University Press, New York, 2000, par. 5.7, 6.10.
- [32] M. A. Nielsen and I. L. Chuang, *Quantum Computation and Quantum Information* (Cambridge University, Cambridge, 2000).
- [33] D.F. V. James, P.G. Kwiat, W.J. Munro, and A.G. White, Phys. Rev. A **64**, 052312 (2001)
- [34] T. Wei, *et al.*, Phys. Rev. A **67**, 022110 (2003).
- [35] M. Barbieri, F. De Martini, G. Di Nepi, and P. Mataloni, Phys. Rev. Lett. **92**, 177901 (2004).
- [36] A. Peres, Phys. Rev. Lett. **77**, 1413 (1996).
- [37] B. Terhal, Lin. Alg. Appl. **323**, 61 (2001).
- [38] M. Lewenstein, B. Kraus, J. I. Cirac, and P. Horodecki, Phys. Rev. A **62**, 052310 (2000).
- [39] M. Lewenstein, B. Kraus, P. Horodecki, and J. I. Cirac, Phys. Rev. A **63**, 044304 (2001).
- [40] D. Bruß, J. I. Cirac, P. Horodecki, F. Hulpke, B. Kraus, M. Lewenstein, and A. Sanpera, J. Mod. Opt. **49**, 1399 (2002).
- [41] G.M. D’Ariano, C. Macchiavello and M.G.A. Paris, Phys. Rev. A **67**, 042310 (2003).
- [42] F. De Martini, V. Bužek, F. Sciarrino, and C. Sias, Nature (London) **419**, 815 (2002).

Figure 1. Schematic layout. Inset: losses simulation by beamsplitter.

Figure 2. Werner weight p versus non-linear parametric gain g . The two-photon density matrices ρ_{th}^{II} are reported for some gain values ($g = 0.1, g = 1, g = 0.3$).

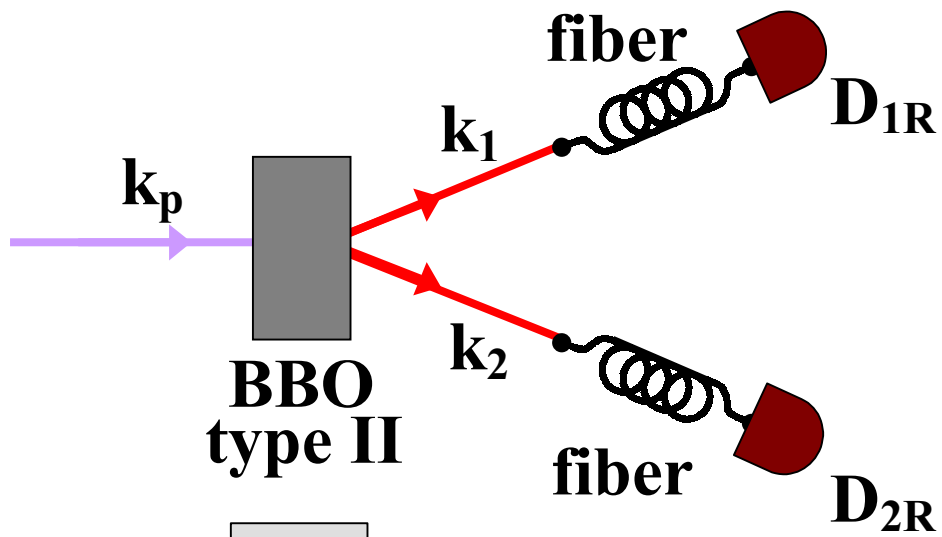
Figure 3. Experimental setup adopted for multiphoton states generation by means of *SPDC* process and characterization by *QST*.

Figure 4. **(a)** Count rates $[D_1]$ as a function of the UV power (arbitrary unit). The continuous line expresses the best fit result. **(b)** Coincidence rates $[D_1, D_2]$ as a function of the UV power.

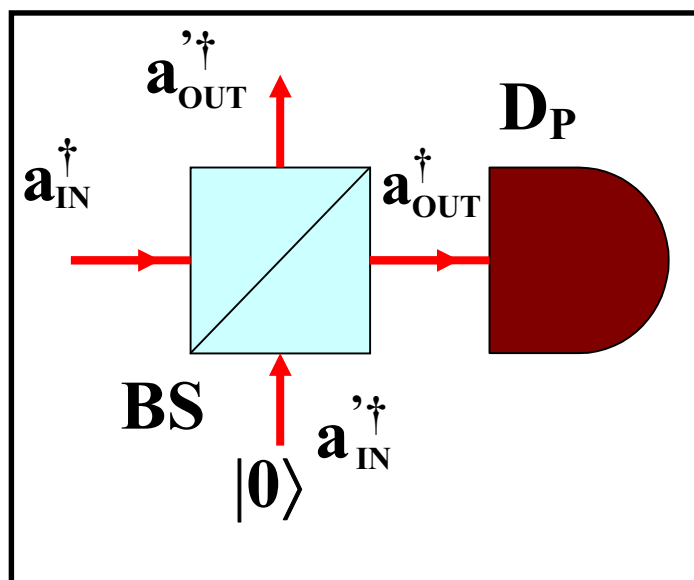
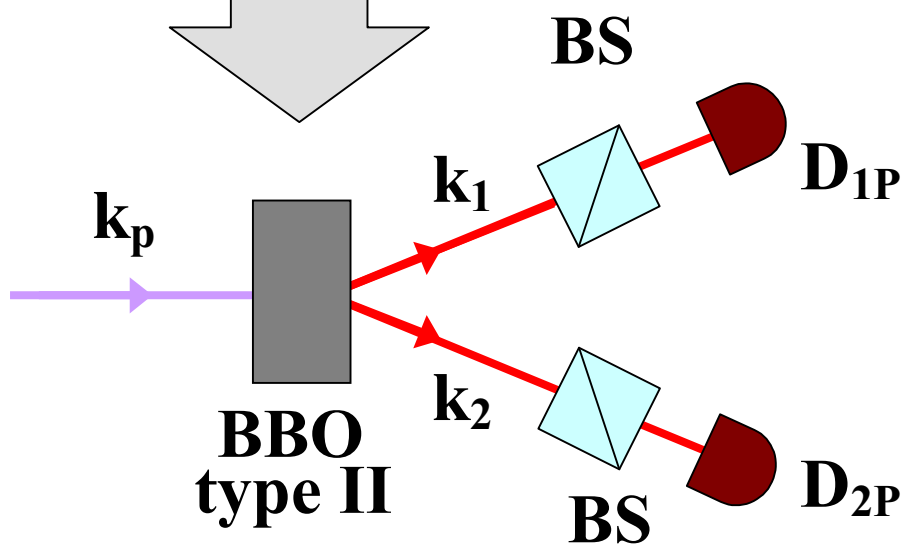
Figure 5. Theoretical ρ_{th}^{II} (left plot) and experimental ρ_{exp}^{II} (right plot) density matrices for different gain values. The experimental density matrices have been reconstructed by measuring 16 two qubits observables through the two tomographic setups $\{T_i\}$. Each tomographic measurement lasted a time t and yielded a maximum twofold counts (cc) for the $|HV\rangle$ projection **(a)** $t = 1$ sec; $cc \simeq 9300$ **(b)** $t = 2$ sec; $cc \simeq 12000$ **(c)** $t = 15$ sec; $cc \simeq 2000$ **(d)** $t = 120$ sec; $cc \simeq 1300$.

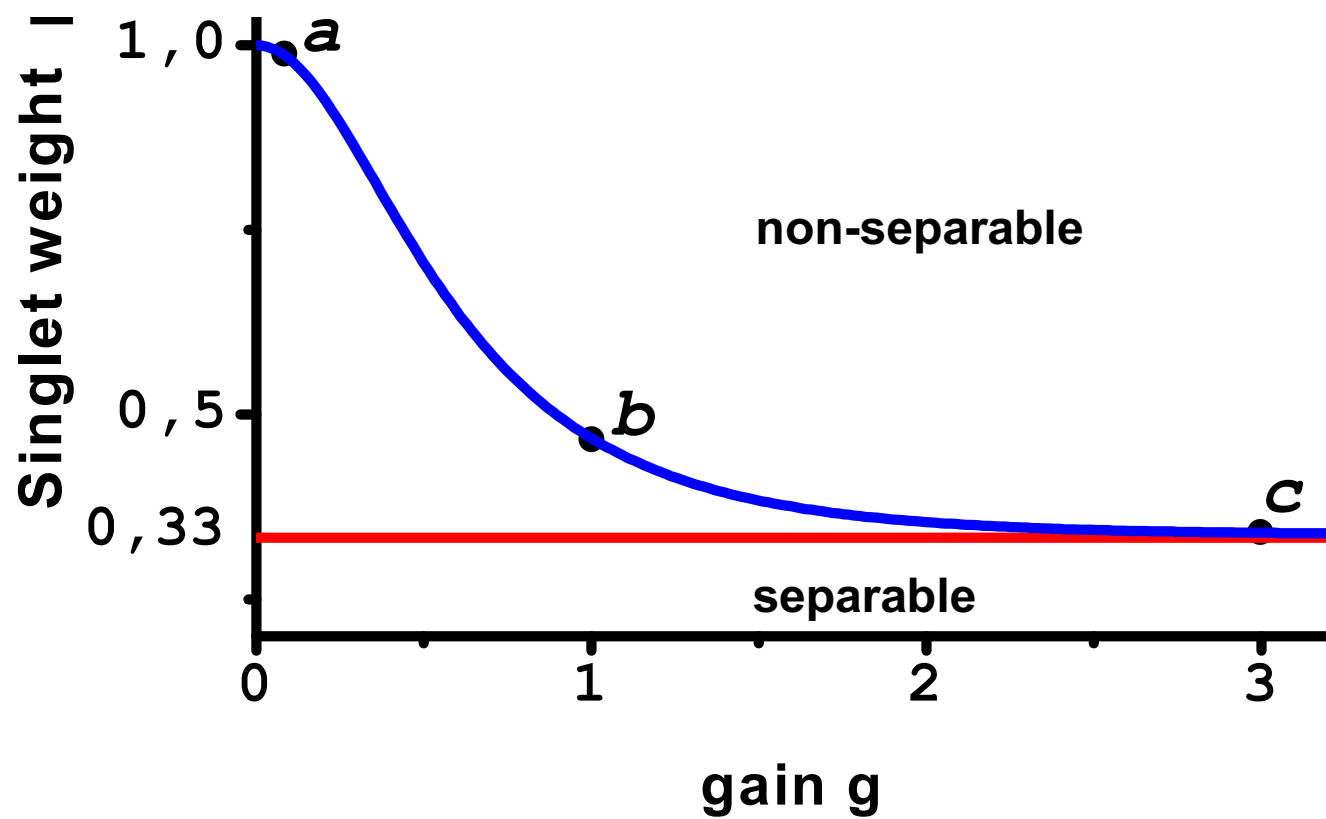
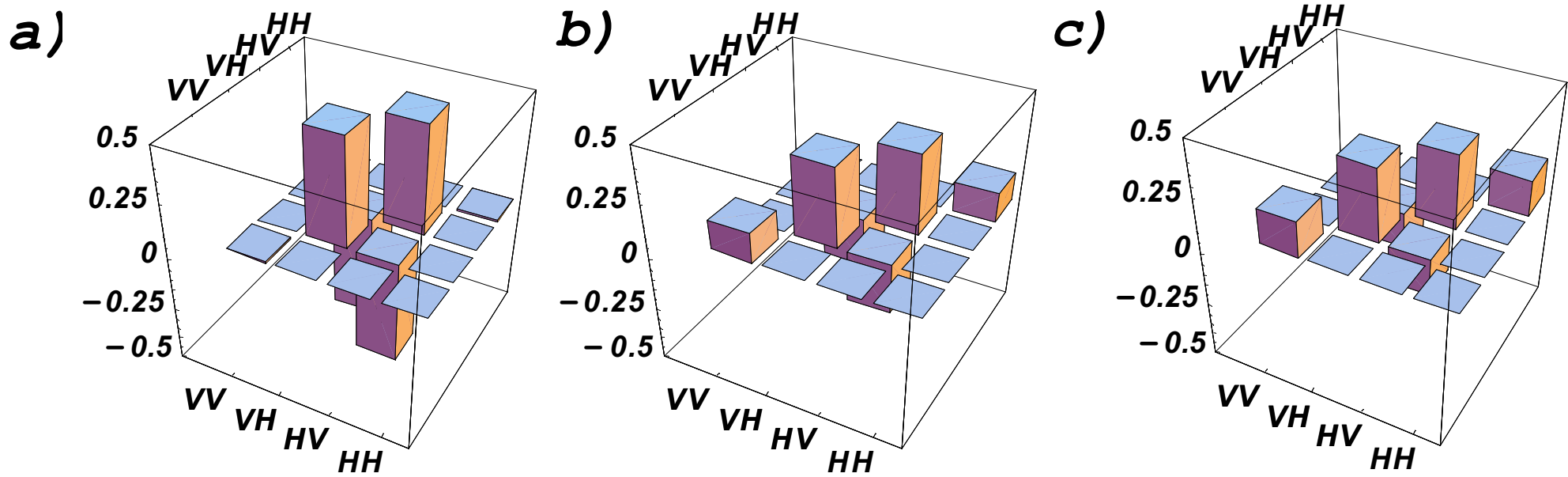
Figure 6.**(a)** The tangle parameter τ in function of the Entropy S of the state. Red line; theoretical plot (13). **(b)** Witness parameter $W = Tr [\hat{O}_W \rho_{exp}^{II}]$ in function of singlet weight p . Red line: theoretical plot (15).

a)

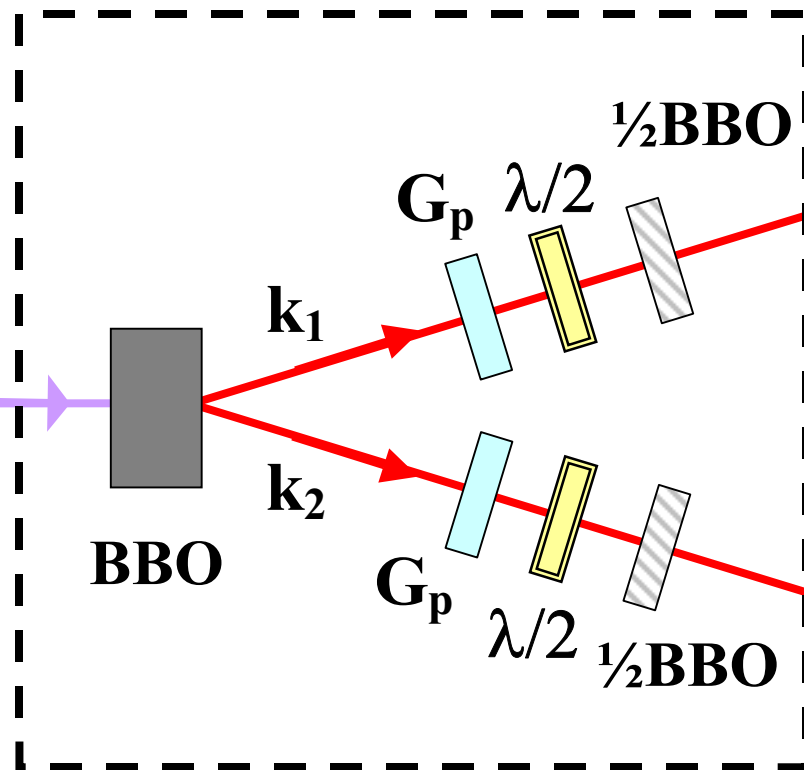


b)

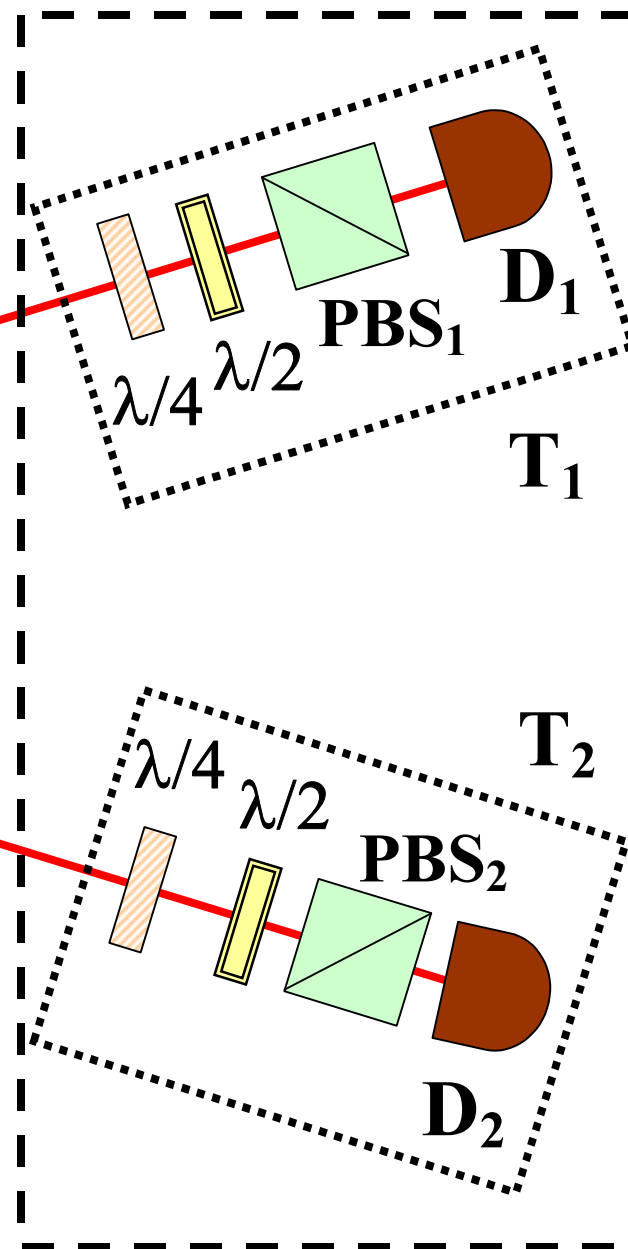




Generation

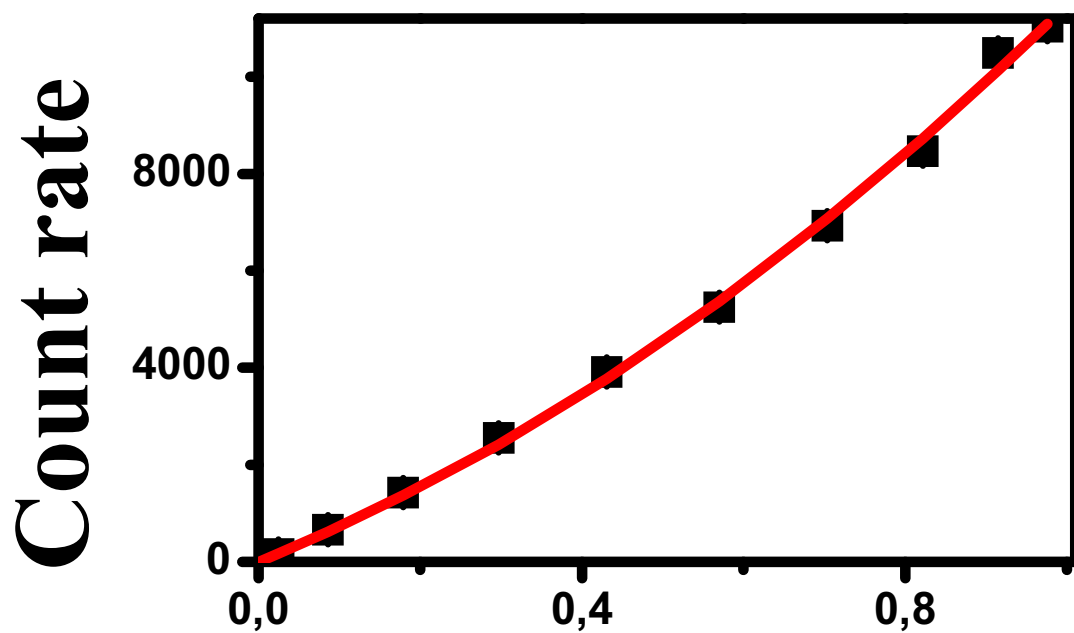


Analysis

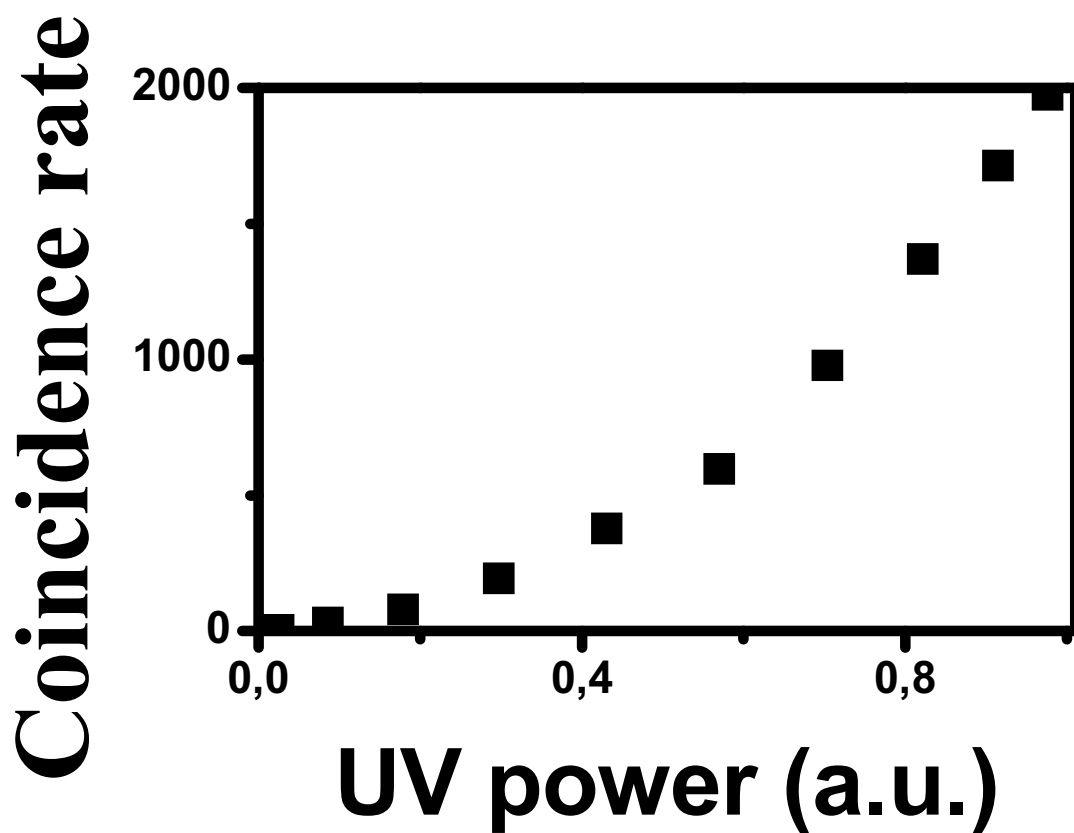


Ti:Sa laser

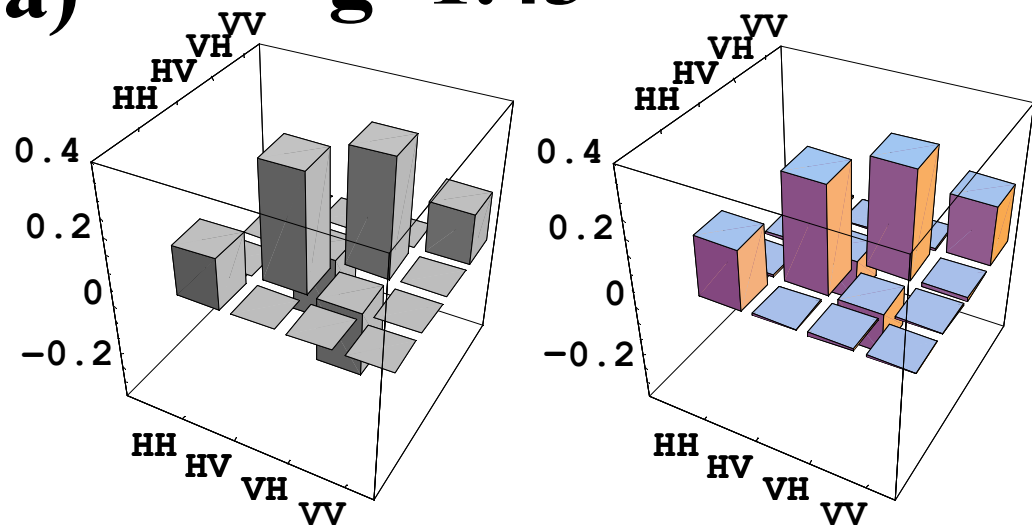
a)



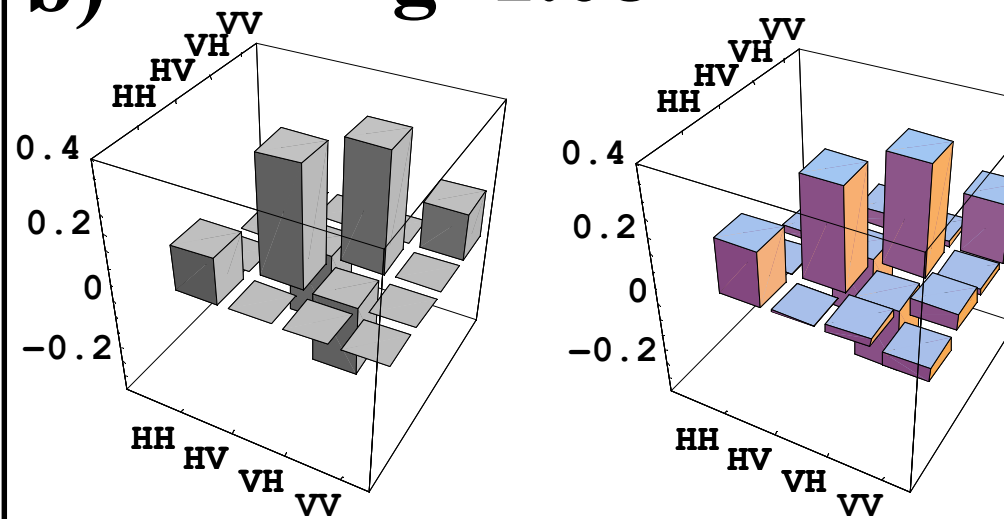
b)



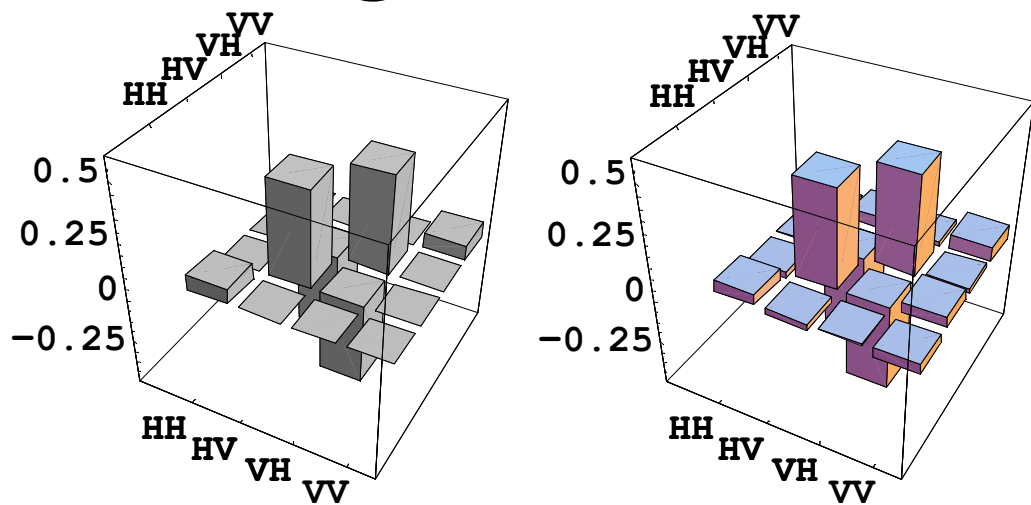
a) $g=1.43$



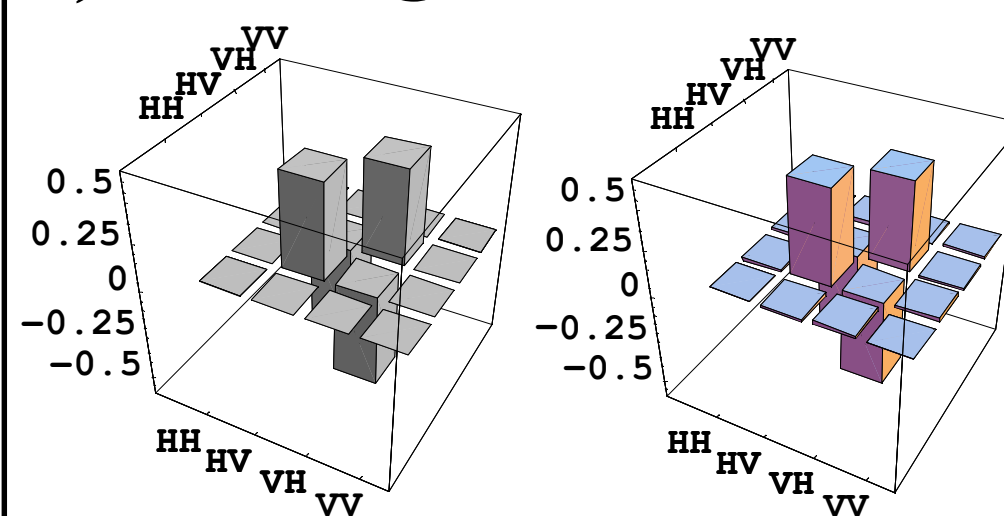
b) $g=1.08$



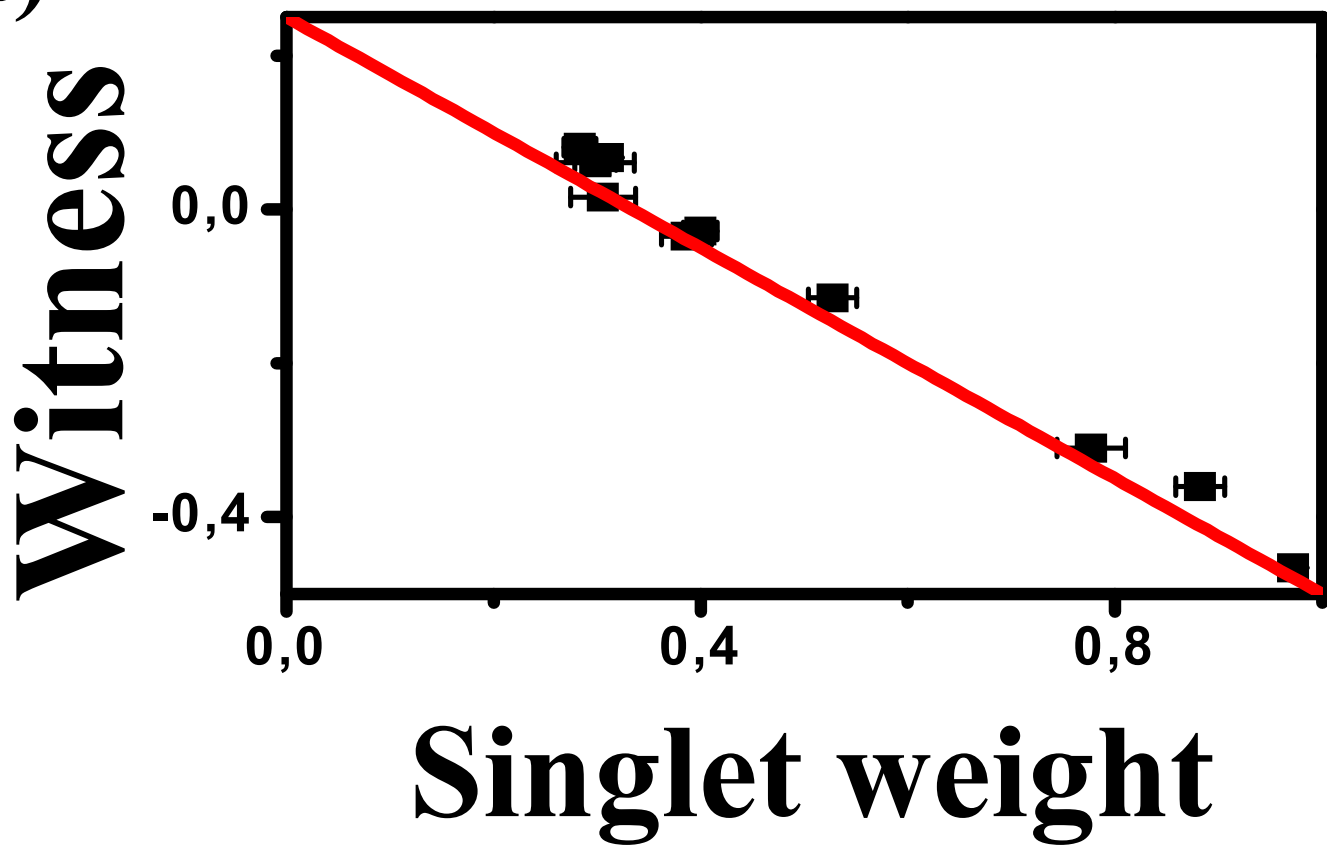
c) $g=0.46$



d) $g=0.05$



a)



b)

